

Chapter 2

Development of an RNA device framework that targets endogenous genes in human cells

Abstract

Ligand-responsive genetic control systems are important tools in synthetic biology. Such tools are especially valuable when they include the capability to regulate endogenous genes. Allosteric ribozyme switches have been designed based on hammerhead ribozymes and RNA aptamers, and have demonstrated programmable ligand-responsive genetic regulation in diverse cell types. We attempted to adapt this class of cis-acting genetic control elements to function in trans. Previous work has demonstrated the division of a cis-acting hammerhead ribozyme into an enzyme strand and a substrate strand that reconstitute catalytic activity upon annealing with one another. We developed a design strategy to divide the allosteric ribozyme switch into two strands, such that the sensor component is entirely contained within the enzyme strand. We investigated the ability of our trans-ribozyme designs to regulate the expression of genes in trans in human cell lines. Cleavage activity of the trans-ribozyme platform was optimized using cis-ribozymes as a model, and our results indicate that the ribozyme stem sequence is not as mutable as previously reported. We verified the cleavage activity of our optimized trans-ribozyme design *in vitro*, and coupled that design to a variety of ancillary genetic elements to direct stability, structure, processing, and localization of the ribozyme transcript *in vivo*. However, we were unable to demonstrate trans-ribozyme-mediated gene silencing, likely due to deficiencies in trans-ribozyme transcript stability and localization.

Introduction

The ability to regulate the expression of endogenous genes is a desired function for synthetic RNA-based control systems. The capability to interact with and modulate endogenous genes enables the silencing of the negative effects of gene products from pathogenic RNA and aberrant messenger RNA (mRNA), forming the foundation for novel gene therapies and tissue engineering methodologies. Such targeted gene silencing has been demonstrated in models of bacterial infection¹, viral infection²⁻⁷, and cancer⁸⁻¹¹. For example, ribozymes have been used to target multiple genes in the HIV genome, effectively inhibiting viral replication in both laboratory studies^{12,13} and clinical trials¹⁴⁻¹⁶. In another example, tumor growth and angiogenesis in a pancreatic cancer mouse model were inhibited by a short hairpin RNA (shRNA) targeting glycogen synthase kinase-3 β , an important serine/threonine protein kinase in tumorigenesis¹¹.

When regulating genes in mammalian cells using synthetic RNA devices, it is often desirable to control the activity of those devices in response to user-specified molecular inputs. This is especially true in the case of cancer therapeutics, where an important strategy to increase the efficacy and safety of the therapy is to target the regulatory effect to diseased cells while leaving healthy cells unaffected. Such ligand-responsive RNA-based genetic control elements have been demonstrated in mammalian cells. In one example, alternative splicing was modulated using switches responsive to cancer biomarkers, such that presence of the biomarker allowed expression of herpes simplex virus-thymidine kinase (HSV-TK), conferring sensitivity to the pro-drug ganciclovir¹⁷. In another example, the balance between proapoptotic and antiapoptotic

genes was controlled using shRNAs containing an aptamer for the archaeal ribosomal protein L7Ae, whose processing was inhibited by ligand binding¹⁸.

There are several desirable features for an effective ligand-responsive gene-regulatory device. Many previously described platforms exhibit some of these key features, but very few exhibit all of them. First, the device must be programmable to respond to different ligand inputs, turning gene expression either on or off in response to ligand binding. Many of the reported ligand-responsive platforms are capable of modulating gene expression either up or down, but not both¹⁹⁻²². Second, the basal level of activity and the switching range of the device must be readily tunable through small alterations to the design to easily adjust device function to application-specific levels. Third, the ligand sensor and gene-regulatory actuator components must be modular in assembly, such that the ligand-binding domain can be easily replaced with a sensor for a different input, and the actuator can be retargeted to regulate a different gene, without necessitating a full and lengthy redesign of the device. Lastly, a device platform that is portable between organisms, such as microbes and higher eukaryotes, can allow for rapid prototyping and optimization of the device in simple organisms and later implementation in more complex organisms. This property is limited to devices that incorporate actuators that do not depend on cell-specific machinery.

RNA control elements derived from the hammerhead ribozyme of the satellite RNA of tobacco ringspot virus (sTRSV)²³ have been demonstrated to exhibit these desired capabilities and thus provide a powerful ligand-responsive platform for mammalian gene regulation. The allosteric ribozyme switch framework developed by Win and Smolke²⁴ demonstrates programmable ligand-responsive genetic regulation

through a synthetic RNA device. These devices transmit ligand sensing by an aptamer component into cleavage of the target gene's mRNA by a ribozyme actuator component, which leads to degradation of the transcript and silencing of gene expression²⁴. The ribozyme switches can be programmed to respond to different ligand inputs through the incorporation of different aptamer sequences²⁴. The activity of ribozyme switches is readily tuned by altering individual nucleotides, which changes the three-dimensional folded state of the device, thus altering the basal level of catalytic activity and the energy difference between the active and inactive conformations. This, in turn, determines the difference in gene expression between the ON and OFF states^{24,25}. The modular components of the ribozyme switch platform can be easily replaced without affecting device activity, and the switch can be placed in the 3' untranslated region (UTR) of any gene of interest to regulate its expression²⁴. Finally, because ribozyme cleavage does not rely on any cell-specific machinery, the platform is highly portable between organisms, supporting rapid prototyping systems that allow designs to be screened in a microbial host such as yeast and optimized designs subsequently ported to mammalian cells with little change in function²⁶.

The primary limitation of the ribozyme switch platform, as with many other previously demonstrated ligand-responsive regulation devices, is that it cannot be used to control endogenous genes^{24,27}. Instead it is limited to the regulation of transgenes, as the cis-acting genetic actuator must be encoded in the region immediately neighboring the target gene. However, previous work has demonstrated that the hammerhead ribozyme can function as two separate molecules, an enzyme strand and a substrate strand, that reconstitute catalytic activity upon annealing with one another^{28,29}. These trans-acting

ribozymes can be tailored to a specific target sequence through the identity of targeting arms that base-pair to regions in the target gene, and can thus be used to target endogenous genes. In an early demonstration, a trans-ribozyme was programmed to target the *gag* gene of HIV-1, lowering levels of that transcript in human cells².

Since this initial demonstration of endogenous gene regulation, investigators have examined factors that determine the functional activity of trans-ribozymes *in vivo*. Trans-ribozymes were found to function far more effectively in the cytoplasm than the nucleus, and localization strategies have been employed to target trans-ribozyme transcripts to the cytoplasm^{30,31}. Taira and colleagues coupled trans-ribozymes to transfer RNA (tRNA) to take advantage of its cytoplasmic localization and stability^{29,31}, and used a random library to screen the region linking the trans-ribozyme and tRNA for increased stability³². Another important factor is the secondary structure of both the trans-ribozyme and target transcripts, which can interfere with binding. In one notable study, a trans-ribozyme was linked to an RNA helicase protein, which removed secondary structure from the target mRNA to allow proper binding and cleavage³³. However, there is disagreement in the field on the effectiveness of trans-ribozymes as gene-regulatory elements, as the studies on trans-ribozymes have rarely included a non-cleaving control trans-ribozyme to clearly demonstrate that observed levels of gene expression knockdown are due to mRNA cleavage from the ribozyme, rather than antisense effects as a result of binding of the trans-ribozyme to the transcript. Indeed, one study investigating trans-ribozymes found that these gene-regulatory elements were no more effective at silencing their target gene than equivalent non-catalytic antisense sequences³.

We attempted to extend the cis-acting ribozyme switch platform developed by Win and Smolke²⁴ to a trans-acting platform capable of regulating the expression of endogenous genes. We divided the allosteric ribozyme switch into an enzyme strand and a substrate strand, such that the sensor component is entirely contained within the enzyme strand. We sought to leverage all of the advantages of the existing cis-ribozyme switch platform while overcoming its limitation of being able to regulate only heterologous genes. We designed three trans-ribozymes and placed their cognate target sequences in the 3' UTR of a fluorescent reporter gene, which we integrated into the chromosome of a human cell line to model the targeting of an endogenous gene. Based on our initial results indicating that the trans-ribozyme designs were unable to silence the target gene, we performed additional studies to optimize the cleavage activity and gene expression knockdown in a model cis-ribozyme architecture, which led to the development of an improved trans-ribozyme design. We also varied the trans-ribozyme expression system, incorporating genetic elements intended to increase the ability of the trans-ribozyme to anneal to and cleave the target strand. Our results indicate that the sequence flexibility of the trans-ribozyme is severely restricted, limiting the capability to design trans-ribozymes to target any gene of choice. We were unable to demonstrate gene regulation *in vivo* from our trans-ribozyme designs, likely due to issues of trans-ribozyme transcript stability and localization.

Results

Design of a trans-ribozyme-based regulatory element in human cells

We first attempted to establish the capabilities of trans-acting RNA devices to regulate endogenous cellular transcripts in human cells. The design of the trans-ribozyme is based on a modification of a hammerhead ribozyme³⁴ that was optimized to enhance cleavage activity in the presence of physiological Mg^{2+} concentrations and hybridization efficiency between the two strands. As shown in Figure 2.1A, the sequence of the hammerhead ribozyme is divided in two at loop I, such that the cleavage site is located in the target transcript. Stems I and III are formed through the hybridization of the ribozyme targeting arms to complementary regions of the target transcript, whereas stem II and loop II are entirely contained within the trans-acting ribozyme strand. This places almost all of the nucleotides reported to be conserved in the enzyme strand, with only the conserved NUX cleavage site in the target strand³⁵. Such designs have shown higher cleavage activity *in vitro* than designs in which the ribozyme is divided at loop II³⁴, and they are more directly adapted to the cis-ribozyme-based RNA device framework²⁴, as any aptamer can then be integrated into loop II. To maintain the tertiary interactions between nucleotides in loops I and II that have been shown to be necessary for catalytic activity at physiological Mg^{2+} concentrations³⁶, stem I of the ribozyme strand contains a bulge that mimics loop I. When the ribozyme strand and target transcript anneal the catalytic core is effectively reconstituted and the target strand is cleaved. Integration of the target sequence in the flexible regulatory space of the 3' UTR of a reporter gene enables knockdown of that gene through targeted cleavage and subsequent degradation of its mRNA (Figure 2.1B).

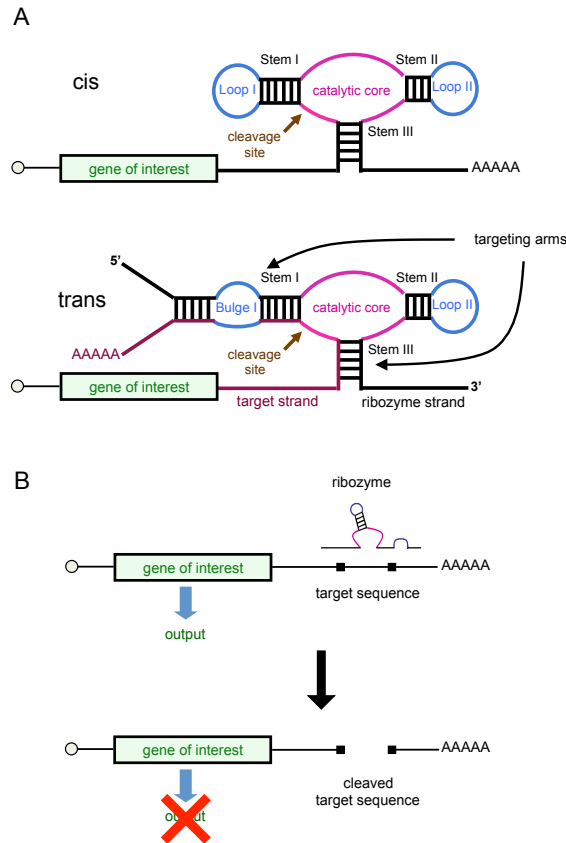


Figure 2.1. Structure and function of the trans-ribozyme. **(A)** The hammerhead ribozyme in cis and trans forms. The catalytic core is shown in magenta, loops and bulges are shown in blue, the ribozyme strand is shown in black, and the target strand is shown in purple. The cleavage site is indicated with an arrow. **(B)** The trans-ribozyme binds and cleaves the target sequence in the 3' UTR of the gene of interest, destabilizing the transcript and reducing protein expression. Partially adapted from Win and Smolke²⁴.

Preliminary studies previously performed in the Smolke laboratory focused on the optimization of trans-ribozyme activity under physiological conditions. *In vitro* experiments on a trans-ribozyme derived from the sTRSV hammerhead ribozyme demonstrated that the length of the targeting arms significantly impacts hybridization

interactions, and therefore cleavage rate, at physiological Mg^{2+} concentrations. Specifically, cleavage activity was shown to be highest when the targeting arm 5' of bulge I and the stem III targeting arm are 16 and 7 base pairs long, respectively. Preliminary experiments conducted in yeast showed limited trans-ribozyme activity (Kate Galloway, unpublished results), but we hypothesized that design modifications would allow higher activity to be achieved in human cells.

The trans-ribozyme molecular design strategies address challenges in the cleavage activity and hybridization efficiency in adapting the unimolecular cis-acting system to the bimolecular trans-acting system. However, in implementing a trans-ribozyme in a cellular system the next level of design must address the stability and localization of the trans-acting molecule, two critical factors in the efficacy of trans-acting RNA regulatory systems. Preliminary experiments previously conducted in the Smolke laboratory have demonstrated that these two factors limit the regulatory activity of trans-ribozymes in yeast cells (Kate Galloway, unpublished results). However, it is likely that differences in the time scales of RNA transcription, processing, trafficking, and degradation may allow trans-ribozymes to function more effectively in human cells than in yeast.

Three trans-ribozymes were designed and tested in human cells (Figure 2.2). Two of the trans-ribozymes are derived from previously studied³⁴ hammerhead ribozymes: sTRSV and peach latent mosaic viroid (PLMVd). The third trans-ribozyme is based on the core of PLMVd but has modified stems designed to target a sequence within the coding region of a yeast-enhanced green fluorescent protein (yEGFP). The trans-ribozymes are flanked immediately upstream and downstream by small hairpins, intended to insulate the trans-ribozyme sequence from the surrounding transcript and prevent

intramolecular binding of the targeting arms, which must remain single-stranded in order to bind to the target sequence. Each trans-ribozyme is coupled with a unique targeting sequence, such that hybridization of the targeting arms reconstitutes stems I and III, forming a catalytically active ribozyme. The targeting sequences are placed within the 3' UTR of EGFP such that cleavage can be detected by monitoring fluorescence levels. Additionally, the targeting sequences are placed in multiple copies within the 3' UTR in order to examine the regulatory activity of the trans-ribozymes as a function of the number of target sites.

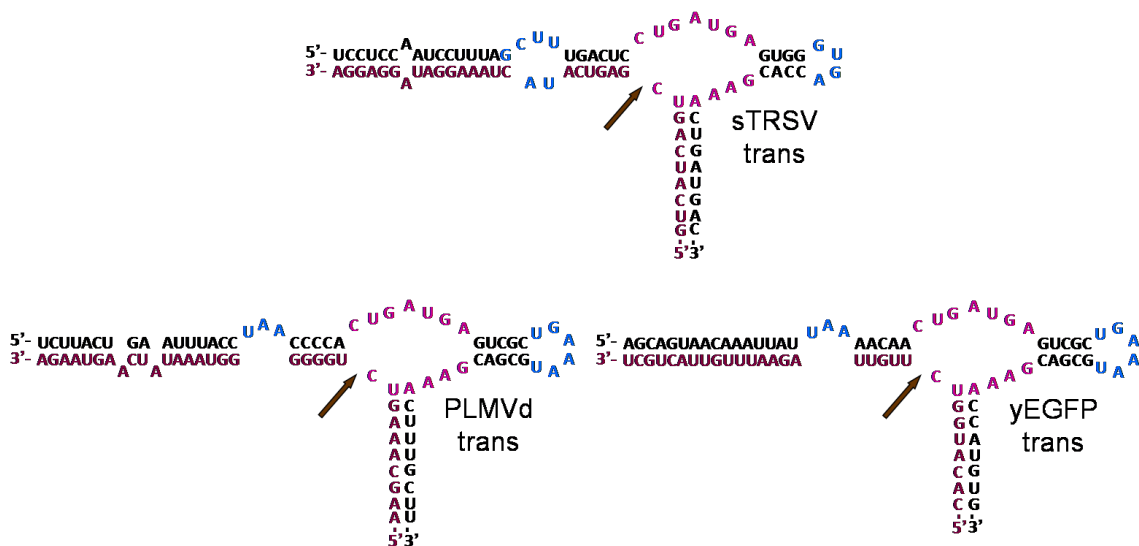


Figure 2.2. Structures of trans-ribozymes bound to target sequences. Coloring is the same as in Figure 2.1.

Characterization of initial trans-ribozyme designs in a human cell line

The trans-ribozymes are expressed from either a cytomegalovirus (CMV) RNA polymerase II (Pol II) or a U6 RNA polymerase III (Pol III) promoter. Pol II promoters

generally control the synthesis of mRNAs, which are capped on their 5' ends with 7-methylguanosine and polyadenylated on their 3' ends. The 5' cap and poly(A) tail associate with one another through a complex of proteins, thereby forming a circular messenger ribonucleoprotein (mRNP) complex that exhibits greater resistance to decapping enzymes and thus increased stability. In contrast, Pol III promoters generally control the synthesis of small non-coding RNAs, such as microRNAs (miRNAs) and small interfering RNAs (siRNAs), and do not have a 5' cap or poly(A) tail. The trans-ribozyme gene is assembled on a plasmid containing the fluorescent reporter gene DsRed-Express, which enables gating for cells that have been transfected with the plasmid (Figure 2.3).

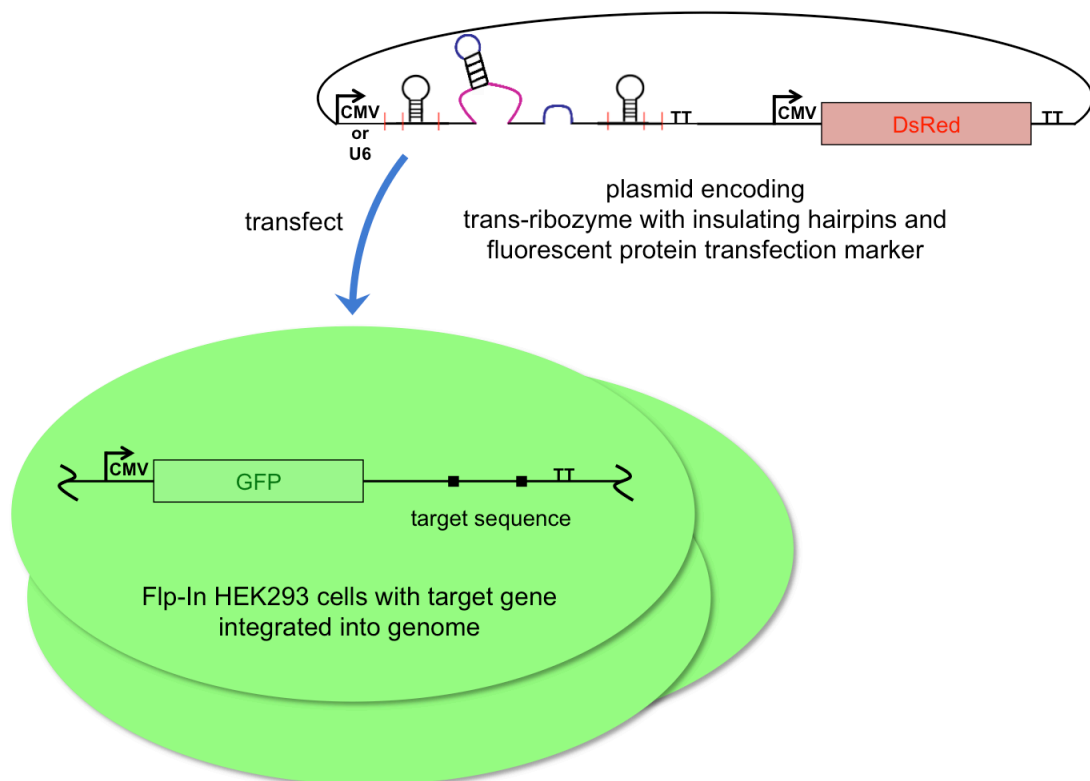


Figure 2.3. Trans-ribozyme and target gene characterization system. The trans-ribozyme is inserted between two insulating hairpins in a multiple cloning site (red lines). The resulting plasmid is transfected into cells with EGFP and the target sequence stably integrated into the genome.

EGFP and the target sequence(s) in its 3' UTR are stably integrated into the genome of human embryonic kidney 293 (HEK293) cells using the Flp-In system to generate isogenic stable cell lines (Figure 2.3). The gene is inserted into a plasmid backbone containing a Flp Recombination Target (FRT) site, thus allowing stable integration through genetic recombination in cell lines that have been engineered to contain a single copy of the FRT site in their genome. Integrating the fluorescent reporter gene in this way enables effective modeling of the targeting of endogenous transcripts by exogenous trans-ribozymes.

To quantify trans-ribozyme regulatory activity, stable cell lines expressing GFP with target sequence(s) were transiently transfected with a plasmid encoding a trans-ribozyme (Figure 2.3). GFP fluorescence was measured using flow cytometry, gating for transfected cells so that only cells harboring the plasmid encoding a trans-ribozyme were analyzed. Decreased GFP fluorescence is expected to correlate with increased regulatory activity. Analysis of the fluorescence of stable cell lines demonstrates that GFP constructs containing one copy of the target sequence are expressed at a higher level than GFP constructs containing multiple (2x or 4x) copies (Figure 2.4). These results indicate that the presence of target sequences in the 3' UTR may have some nonspecific effect on the expression of the target gene, potentially through transcript destabilization or

translational efficiency. However, even with these nonspecific effects, the data clearly indicate that none of the trans-ribozyme designs are able to downregulate expression of the target gene in this assay (Figure 2.4).

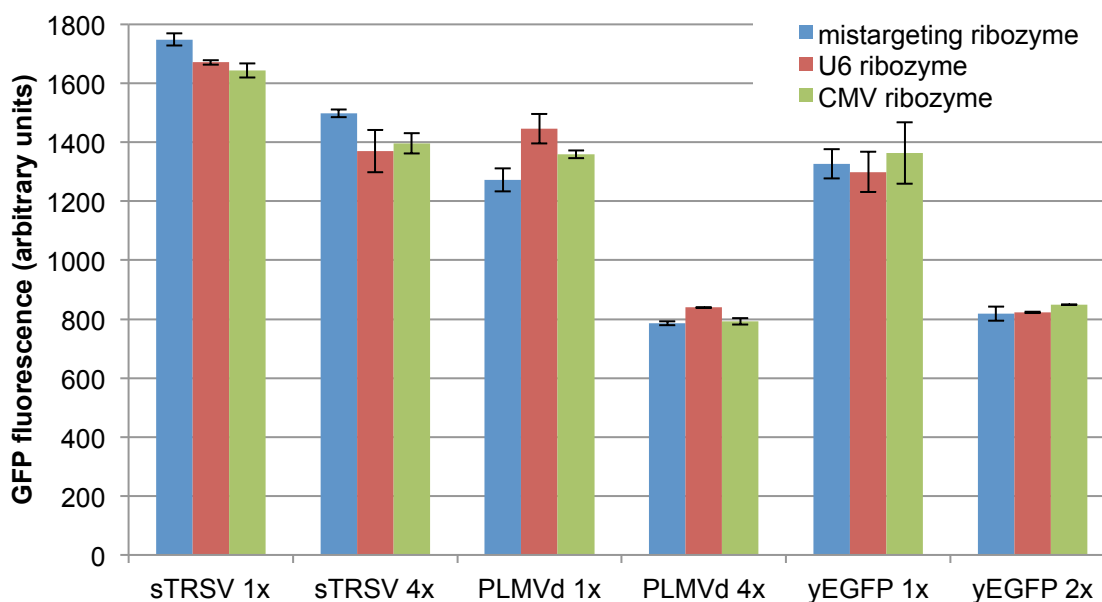


Figure 2.4. Activity of trans-ribozymes. GFP fluorescence levels are reported for stably integrated constructs encoding one or multiple copies of trans-ribozyme target sequences transfected with constructs encoding trans-ribozymes. Mistargeting trans-ribozymes that do not bind to the target sequence are included for comparison. Reported values are geometric mean \pm s.d. from biological duplicates.

There are two possible explanations for why the trans-ribozymes do not exhibit gene silencing activity. One possibility is that the two strands may not properly anneal *in vivo* to form a catalytically active ribozyme. A second possibility is that although the two strands properly anneal, the ribozyme as formed does not cleave at a sufficient rate to downregulate gene expression. It has previously been demonstrated that ribozyme

cleavage rate is correlated with *in vivo* gene knockdown³⁷, and specifically that if the cleavage rate is too low then gene regulation will not be observed.

Cis-ribozymes as a model for optimizing *in vivo* cleavage activity

To investigate whether the cleavage rate of the formed trans-ribozyme would be sufficient to observe knockdown *in vivo*, we designed Type I cis-ribozymes based on the sTRSV trans-ribozyme. Such designs remove the variable of whether the two strands can properly anneal in the cell and allow investigation of gene knockdown through ribozyme cleavage. K was formed by adding a GUUG tetraloop to the end of Stem III of the sTRSV trans-ribozyme (Figure 2.5), covalently joining the two strands into one. W is based on K but more closely resembles wild-type sTRSV, and Y even more so; W has the stem III sequence of sTRSV and Y is identical to W but with the loop I sequence reverted to that of wild-type sTRSV. CU is identical to Y except that the distal portion of stem I is integrated into a different position in bulge I. CU LsIII is identical to CU but with stem III extended by four base pairs, and CU LsIII inversion is identical to CU LsIII but with a stem III A-U pair changed to U-A. CK LsI, CK LsIII, and CK LsIV are all identical to CU LsIII but with the sequences of stem I, stem III, or both, respectively, from K. U LsIII is identical to CU LsIII except that the distal portion of stem I is integrated into a different position in bulge I. Finally, HHe-PLMVd is adapted from a previously described trans-ribozyme⁴, and 3-way AA and 3-way AAA are based on CU LsIII but include a three-way junction with an additional helix in stem I³⁸.

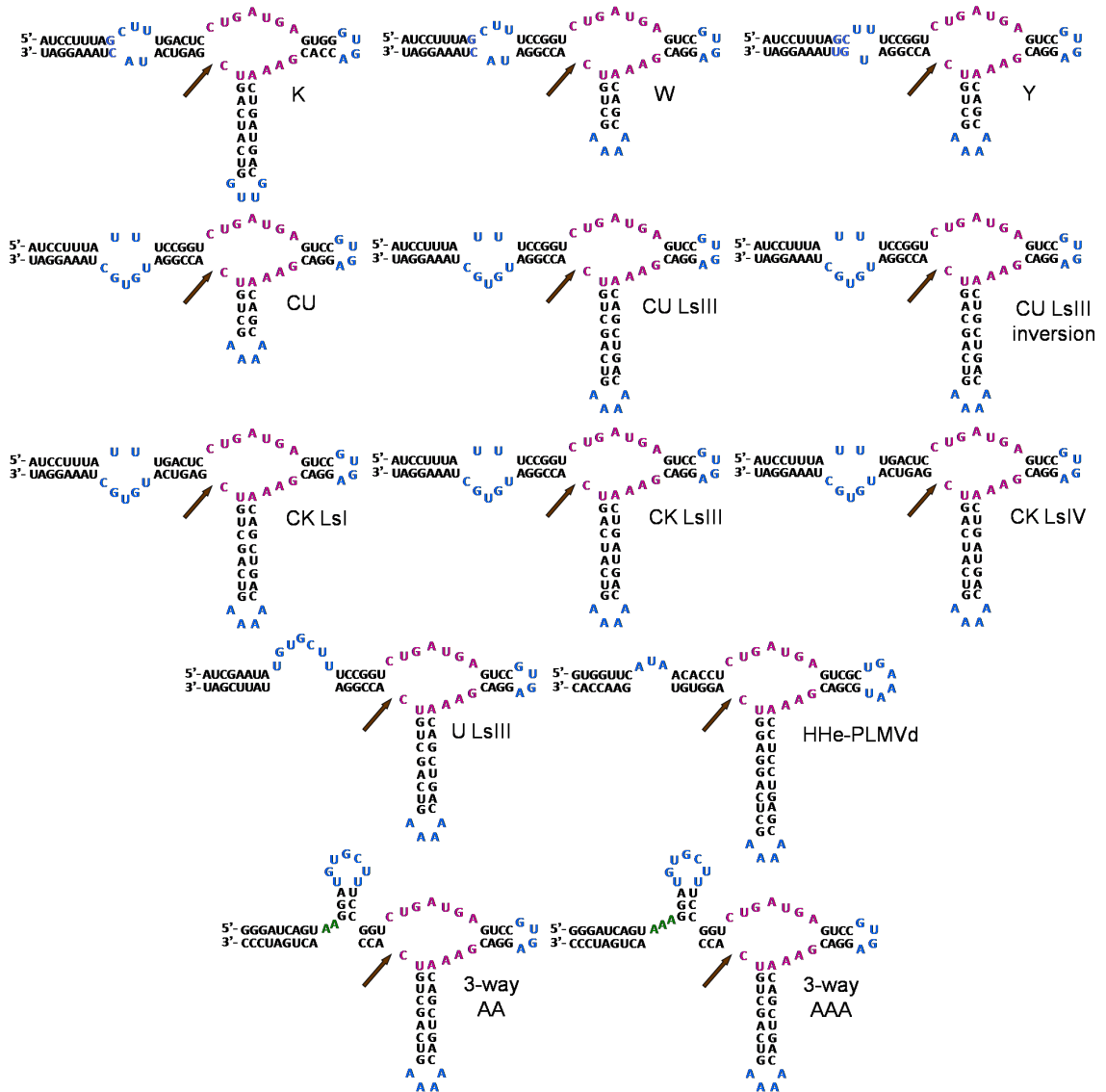


Figure 2.5. Structures of cis-ribozymes used to model trans-ribozyme activity. Stems are shown in black, the catalytic core is shown in magenta, and loops and bulges are shown in blue.

Characterization of Type I cis-ribozymes in a human cell line

Each Type I cis-ribozyme was placed in the 3' UTR of EGFP and gene regulation activity was measured in transient transfection assays by flow cytometry. K exhibited very little activity, with GFP fluorescence 80% of the non-cleaving control (Figure 2.6), indicating that the sTRSV trans-ribozyme would likely not be able to silence its target *in vivo*. The sequence of W is more closely related to wild-type sTRSV and Y even more so, and the activity of these designs reflects this. The alteration of the stem I integration point in CU leads to greater activity, and the extension of stem III in CU LsIII leads to a level of activity approaching that of sTRSV, with 8% expression compared to non-cleaving control. Inversion of the A-U base pair had a small detrimental effect on activity, while the three CK designs exhibited better activity the more similar they were to CU LsIII. Finally, U LsIII and HHe-PLMVd exhibited high levels of regulatory activity, while the 3-way designs showed little activity. These results suggest that the sequences of the ribozyme stems are not as flexible as previously reported^{2,35,39-41}.

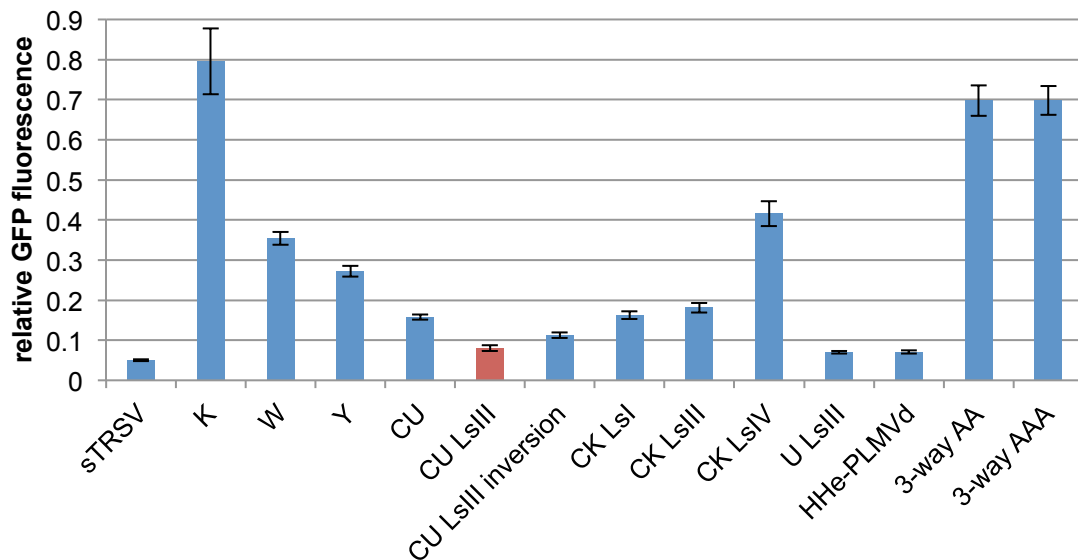


Figure 2.6. Activity of type I cis-ribozymes. Type I cis-ribozymes model the activity of trans-ribozymes. Relative GFP fluorescence levels are reported for transiently transfected constructs encoding ribozyme switch sequences. Reported values are geometric mean \pm s.d. from biological duplicates or triplicates and normalized to the non-cleaving sTRSVctrl.

Development of an improved trans-ribozyme

Based on its high level of gene-regulatory activity CU LsIII was chosen as the basis for a new trans-ribozyme design (Figure 2.7A). *In vitro* cleavage assays were performed to confirm the binding activity of the CU LsIII trans-ribozyme. For these experiments, the trans-ribozyme and target strands were synthesized using *in vitro* transcription, purified, and denatured and renatured separately. The RNA strands were then incubated together in a buffer representative of physiological conditions (500 μ M MgCl₂, 100mM NaCl, 50mM Tris-HCl (pH 7.5) at 37°C). Under these assay conditions, CU LsIII exhibited a cleavage rate of $\sim 0.3 \text{ min}^{-1}$ (Figure 2.7B), which is comparable to the cleavage rates of other ribozyme switches successfully used to regulate gene expression in yeast and mammalian cells^{25,26}. The results suggest that the CU LsIII trans-ribozyme is capable of binding and cleaving its target and should be capable of doing so *in vivo* at a rate sufficient for controlling gene expression levels.

Incorporation of ancillary elements in the trans-ribozyme transcript to direct stability, structure, processing, and localization

There are a number of reasons why the trans-ribozymes described above may not be able to effectively cleave their target transcripts in human cells. The main obstacles are likely the stability of the trans-ribozyme strand in the cellular environment and the ability of this strand to bind to its target strand in the time scale of its lifetime. These issues are related, in that the less time required for the trans-ribozyme strand to bind to its target the less time it needs to exist in the cell, and the higher the stability of the trans-ribozyme strand the more time it will have to bind to its target. To address these issues, we developed a variety of expression constructs incorporating ancillary genetic elements into the sequence context of the CU LsIII trans-ribozyme.

When expressed from the CMV Pol II promoter, the trans-ribozyme is part of a longer transcript. Since the trans-ribozyme may interact with other parts of the transcript in a way that disrupts binding and cleaving of the target strand, we designed a construct containing cis-ribozymes immediately upstream and downstream of the trans-ribozyme and its insulating hairpins (Figure 2.8A). This construct was intended to function by cleaving the trans-ribozyme out of the transcript, potentially making the trans-ribozyme more accessible for binding to the target strand. However, the trans-ribozyme strand may be highly unstable once excised from the rest of the mRNP, so we also designed a construct containing large hairpins internal to the cis-ribozymes (Figure 2.8B). Following cis-ribozyme cleavage these large hairpins are expected to stabilize the 5' and 3' ends of the excised transcript, protecting the trans-ribozyme strand from RNA exonuclease activity. These large hairpins were also tested in constructs without cis-

ribozymes, in both the CMV Pol II and U6 Pol III promoter expression systems (Figure 2.8C).

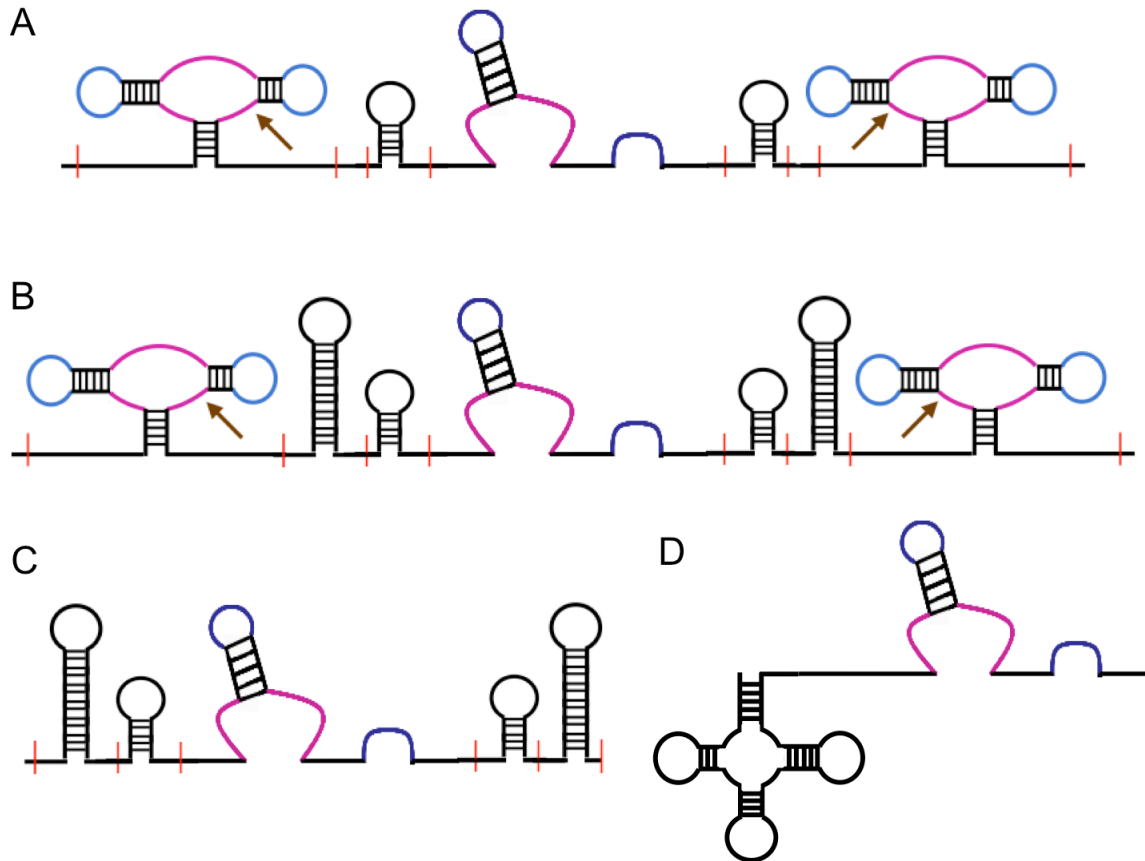


Figure 2.8. Trans-ribozyme ancillary elements. **(A)** Cis-ribozymes cleave the trans-ribozyme (with its insulating hairpins) out of the larger transcript. **(B)** Large hairpins stabilize the ends of the trans-ribozyme strand after excision. **(C)** Large hairpins stabilize Pol II and Pol III trans-ribozyme transcripts. **(D)** tRNA^{Val} stabilizes the trans-ribozyme transcript and localizes it to the cytoplasm.

Alternatively, we inserted tRNA^{Val} immediately upstream of the trans-ribozyme (Figure 2.8D), adapting work from Koseki and colleagues²⁹. They demonstrated that

their chimeric tRNA trans-ribozymes were highly stable in human cells and localized to the cytoplasm, and were able to cleave HIV-1 RNA *in vivo*³¹. We attempted to reproduce their work in our experimental system, using their HIV-targeting Rz2, as well as replacing the HIV trans-ribozyme with CU LsIII.

We assayed the ancillary elements with flow cytometry using transient transfections of stable lines as described above (Figure 2.3). None of the ancillary elements conferred activity on the CU LsIII trans-ribozyme (Figure 2.9). Additionally, we were unable to reproduce the activity of the HIV tRNA trans-ribozyme reported by Koseki and colleagues. We hypothesized that the stability of the GFP reporter used in our studies might be too high, such that significant protein levels remain even when the associated mRNA is cleaved by trans-ribozymes, masking the knockdown effect. To address this possibility, we replaced GFP with destabilized enhanced GFP (d2EGFP)⁴², which has a much shorter half-life than its parent. However, this modification to the experimental system did not result in detectable trans-ribozyme activity.

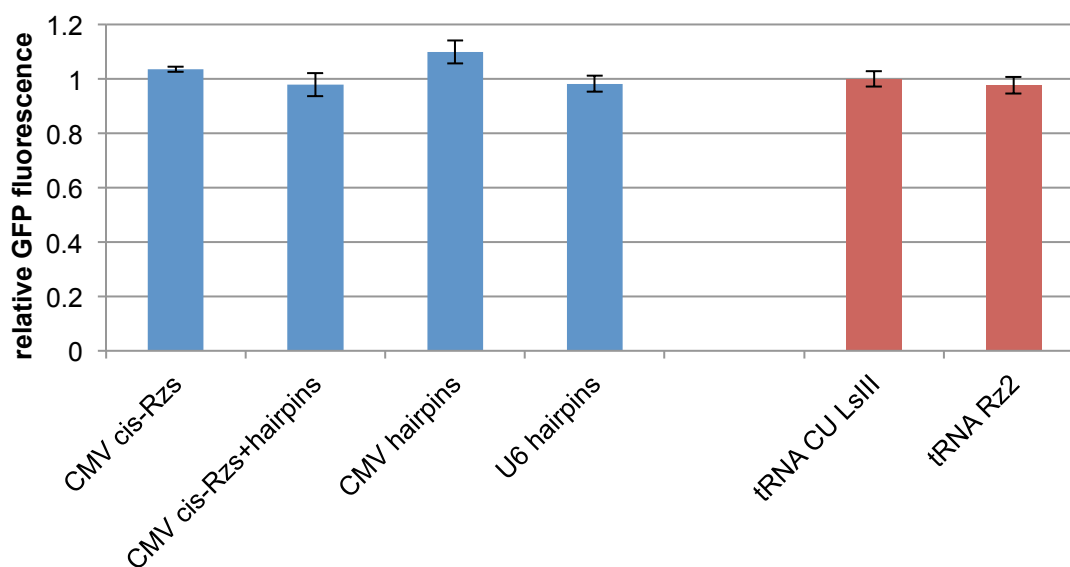


Figure 2.9. Activity of trans-ribozymes with ancillary elements. GFP fluorescence levels are reported for stably integrated constructs encoding trans-ribozyme target sequences transfected with constructs encoding trans-ribozymes with ancillary elements. Reported values are geometric mean \pm s.d. from biological duplicates and normalized to non-cleaving control trans-ribozymes.

Discussion

We attempted to develop a trans-acting version of the cis-acting ribozyme switch platform previously developed in the Smolke laboratory²⁴. Our trans-ribozyme architecture benefits from the previous engineering efforts directed to the cis-acting platform, in particular the design principles for aptamer integration with the ribozyme to build functional ligand-responsive gene-regulatory devices. The trans-ribozyme switch platform should have the added advantage of being able to regulate endogenous gene targets in trans in response to specified molecular inputs. However, there are additional requirements for such a trans-acting RNA device to function properly. Specifically, the functional RNA must be expressed in the cell at an appropriate concentration and localized appropriately, the binding site on the mRNA target must be accessible, and once annealed the duplex must fold into a catalytically active conformation.

Since we did not observe gene-regulatory activity from our initial trans-acting ribozyme designs (Figure 2.4), we first examined the ability of our designs to exhibit cleavage activity when annealed to the target sequence. Specifically, we constructed and

characterized cis-ribozyme versions of our trans-ribozyme designs, which were more likely to fold into the desired conformation based on the unimolecular context. Indeed, the cis version of the sTRSV trans-ribozyme exhibited minimal regulatory activity (Figure 2.6). We investigated the effects of stem length, stem and loop sequence, and loop I integration position on *in vivo* activity. We found that deviation from the sTRSV sequence in the ribozyme stems was detrimental to ribozyme function (Figure 2.6). This was surprising given that the stem sequence has generally been considered to be mutable due to its sequence diversity among natural hammerhead ribozymes, unlike the highly conserved catalytic core^{35,39-41}. These investigations led to the design of a new trans-ribozyme with a high degree of sequence similarity to sTRSV, which we used for all subsequent device optimization.

Following development of the optimized trans-ribozyme design, we further explored modifications to the design of the expression system that would support a high level of expression of the trans-ribozyme transcript. In particular, the transcription rate of the trans-ribozyme expression system was set to a high level by testing two strong promoters that act through different mechanisms, the CMV (Pol II) and U6 (Pol III) promoters. We further introduced design elements to reduce the degradation rate of the trans-ribozyme transcript by incorporating large hairpins on the 5' and 3' ends of the Pol III transcript and the unprotected portion of the Pol II transcript following excision from the mRNP mediated by cis-ribozymes. We also used a chimeric tRNA trans-ribozyme expression platform, which had previously been demonstrated to support gene regulation from a trans-ribozyme and shown to have a long half-life *in vivo*²⁹.

In addition to being present in cells at a sufficiently high concentration, a functional trans-ribozyme must also be localized to the same subcellular location as its target to be able to bind and cleave. Co-localization of the trans-ribozyme and target strands has been shown to be important for activity³, and we hypothesized that the chimeric tRNA trans-ribozymes would be transported to the cytoplasm, increasing their local concentration in the vicinity of their target mRNA and thereby improving hybridization efficiency. We incorporated hairpins immediately upstream and downstream of the trans-ribozyme to insulate it from the surrounding transcript, attempting to minimize misfolding that would occlude the targeting arms. We demonstrated with *in vitro* cleavage assays that the trans-ribozyme is capable of annealing with and cleaving its target sequence under physiological conditions (Figure 2.7).

Despite optimization of cleavage activity in model cis-ribozymes and incorporation of design elements to increase trans-ribozyme stability *in vivo*, we were unable to demonstrate trans-ribozyme-mediated gene-regulatory activity (Figure 2.9). We demonstrated with model cis-ribozymes that cleavage activity was sufficiently high to produce a large amount of gene knockdown, and we showed that the *in vitro* cleavage activity of our improved trans-ribozyme was comparable to that of previously characterized *in vivo* functional cis-ribozymes in yeast and mammalian systems. Taken together these results suggest that our trans-ribozyme did not function *in vivo* due to issues with transcript levels and co-localization with the target strand. Our efforts to improve trans-ribozyme stability and localization did not resolve these issues.

One possible area for further investigation is target site accessibility, which we did not address with any of our designs. It has been shown that in a typical mRNA many target sites will be inaccessible due to secondary and tertiary structure^{33,35}. Optimization of target site location within the target mRNA strand could lead to functional trans-ribozymes. However, successful regulation of an endogenous gene could require extensive screening of many trans-ribozymes targeting different target sites. Another possible strategy is employing RNA localization elements to target trans-ribozyme transcripts to the specific subcellular location of the mRNA target^{43,44}, increasing the local effective concentration and increasing the likelihood of hybridization between the two strands.

The finding that the sequence of the ribozyme stems is less flexible than expected coupled with the issue of target site accessibility severely limits the capability of trans-ribozymes to target endogenous genes. Furthermore, the independence of trans-ribozymes from cell-specific machinery makes them vulnerable to degradation, while other methods for regulating endogenous genes, such as miRNA⁴⁵ and clustered regularly interspaced palindromic repeats interference (CRISPRi)⁴⁶, benefit from protein complexes that protect the RNA and facilitate interaction with the target strand. Taken together, the limitations of the trans-ribozyme platform present a significant challenge to the regulation of endogenous genes, while other RNA-based platforms are more effective and promising. Ligand-responsive miRNAs have previously been demonstrated⁴⁵, and although allosteric regulation has not yet been demonstrated for CRISPRi, such capability may soon be realized. These platforms may therefore be better poised to provide programmable ligand-responsive regulation of endogenous genes.

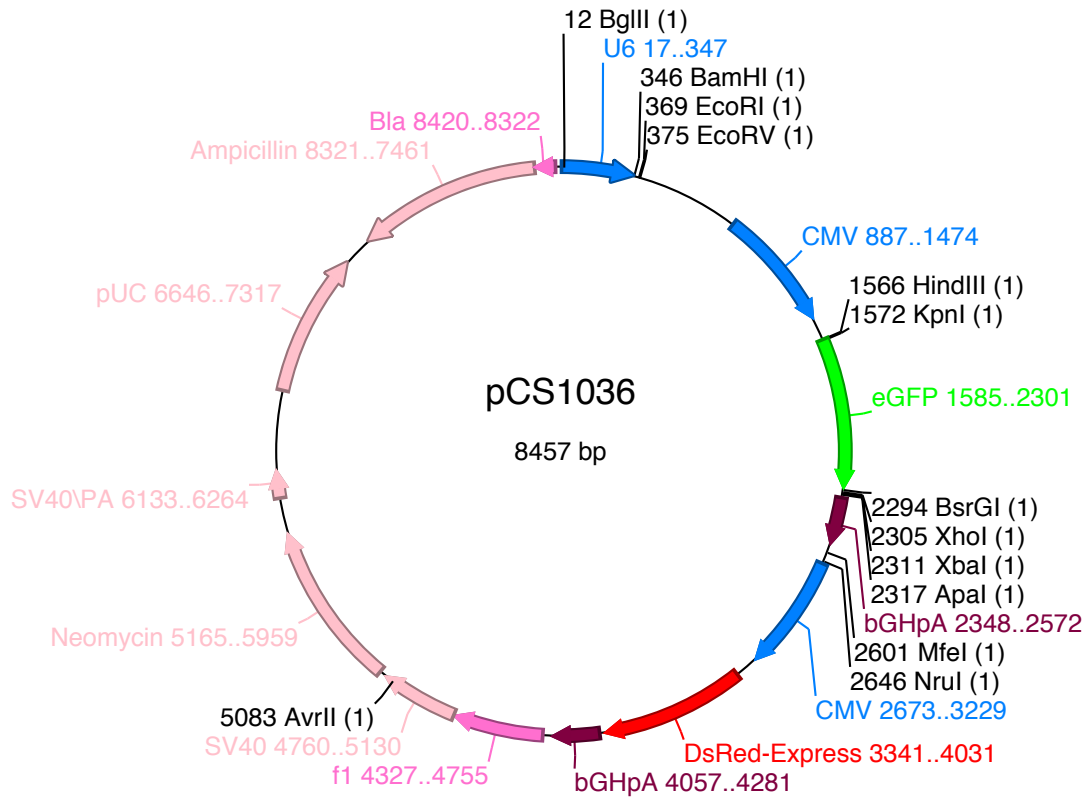
Methods

Plasmid construction

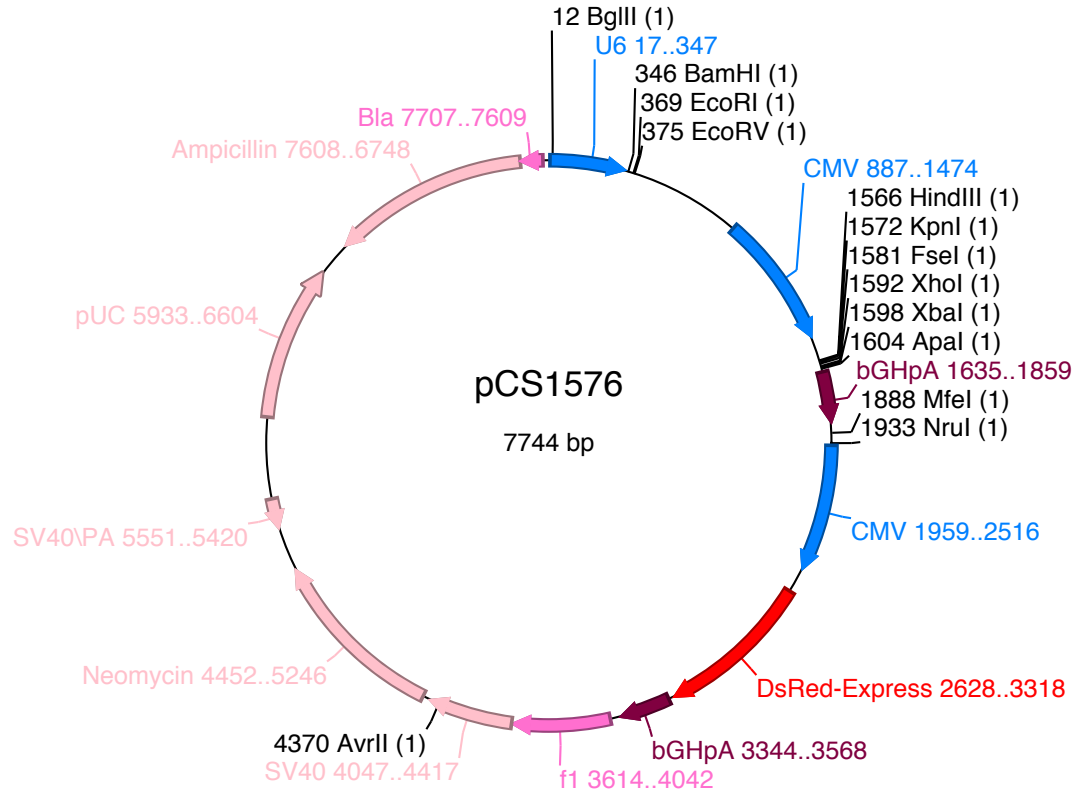
All plasmids were constructed using standard molecular biology techniques. Oligonucleotides were synthesized by Integrated DNA Technologies and the Stanford Protein and Nucleic Acid Facility. Cloning enzymes, including restriction enzymes and T4 DNA ligase, were obtained from New England Biolabs. Ligation products were electroporated into *Escherichia coli* DH10B (Life Technologies) using a GenePulser XP (Bio-Rad Laboratories) system using standard methods. Clones were screened using colony polymerase chain reaction (PCR) and verified by sequencing (Laragen Inc. and Elim Biopharmaceuticals). 15% glycerol stocks were made from *E. coli* in logarithmic growth phase and stored at -80°C .

A standardized cloning method was developed to facilitate insertion of trans-ribozymes into various sequence contexts. The DNA fragment insertFseI was inserted into pCS1036 (courtesy Yvonne Chen) (derived from pcDNA3.1(+) (Life Technologies)) between the restriction sites KpnI/XhoI to form pCS1576 (Figure 2.10), which contained a U6 and a CMV promoter for expressing trans-ribozymes and DsRed-Express as a transfection control. Cassettes containing restriction sites, a terminator (U6 only), and small hairpins designed to prevent intramolecular binding of the trans-ribozyme targeting arms (U6 trans-ribozyme cassette and CMV trans-ribozyme cassette) were inserted downstream of the U6 (between BamHI/EcoRI) and CMV (between FseI/XhoI) promoters to form pCS1646 and pCS1662, respectively (Figure 2.10). Ancillary cis-ribozymes were inserted into pCS1662 between HindIII/KpnI and XbaI/ApaI to form pCS1955. Ancillary large stabilizing hairpins were inserted into pCS1646 between

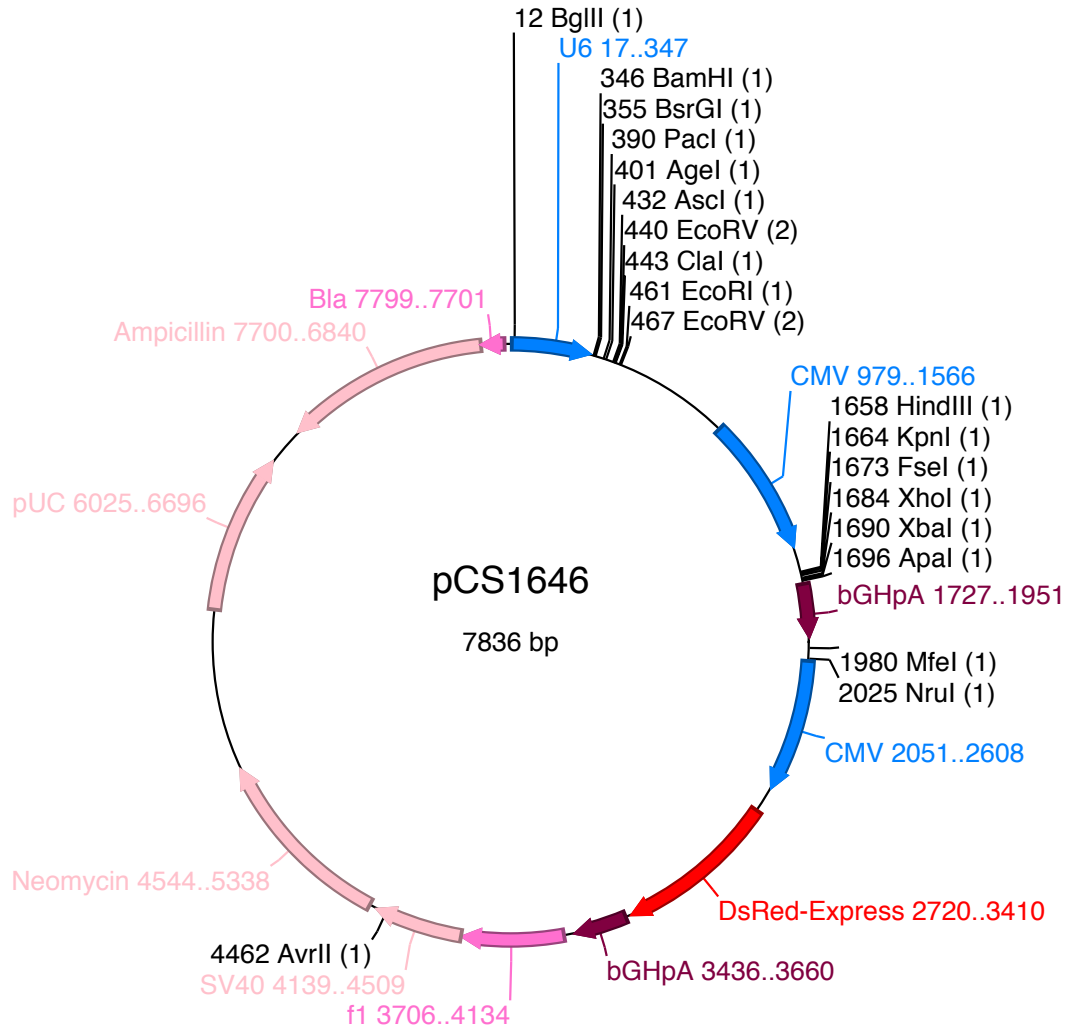
BamHI/BsrGI and AscI/ClaI and into pCS1662 between KpnI/FseI and XhoI/XbaI to form pCS1953 and pCS1954, respectively. Both ancillary cis-ribozymes and large stabilizing hairpins were inserted into pCS1662 (using the same restriction sites used to form pCS1955 and pCS1954) to form pCS1956. Trans-ribozymes were inserted into pCS1646, pCS1662, pCS1955, pCS1953, pCS1954, and pCS1956 between PacI/AgeI.

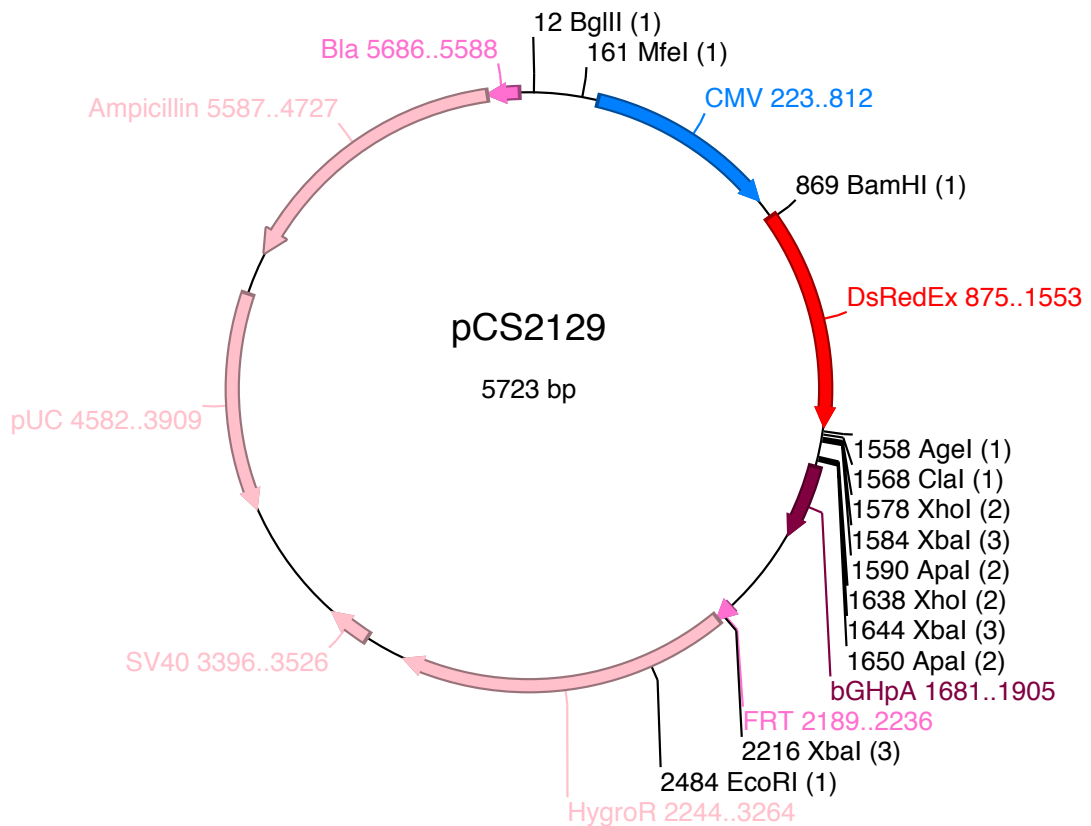
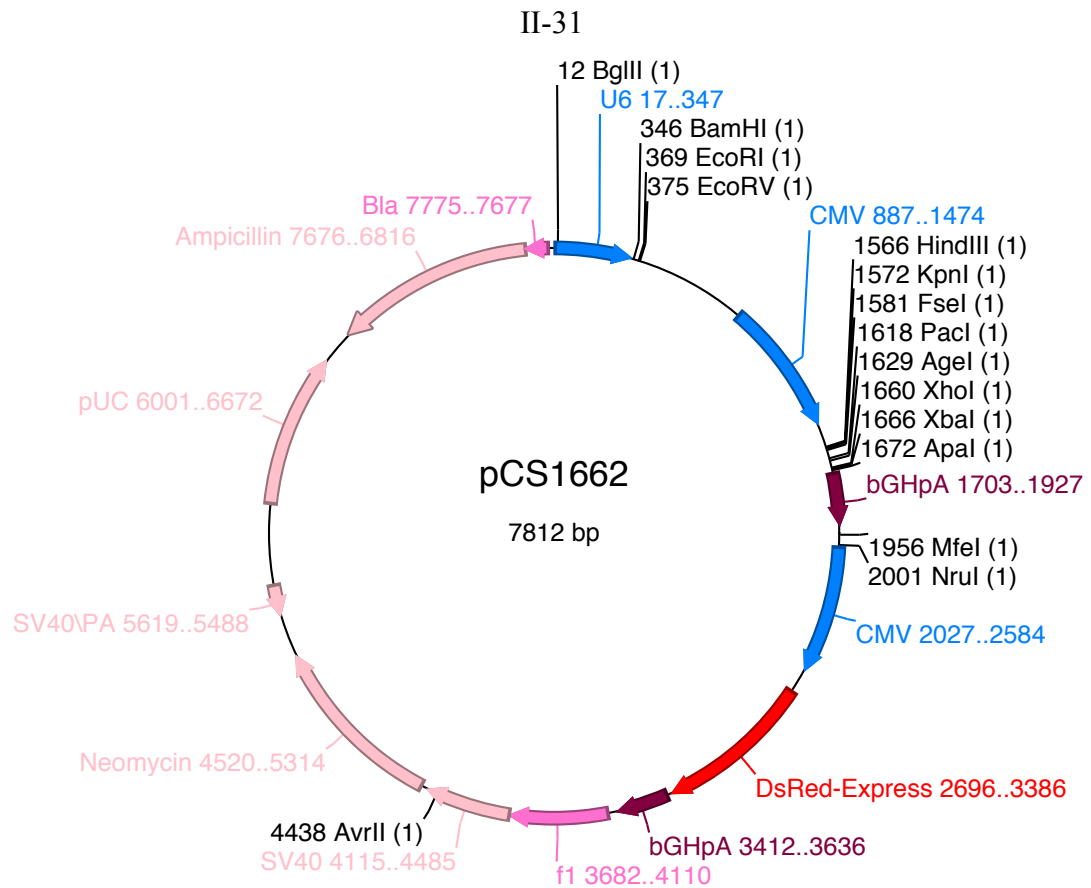


II-29



II-30





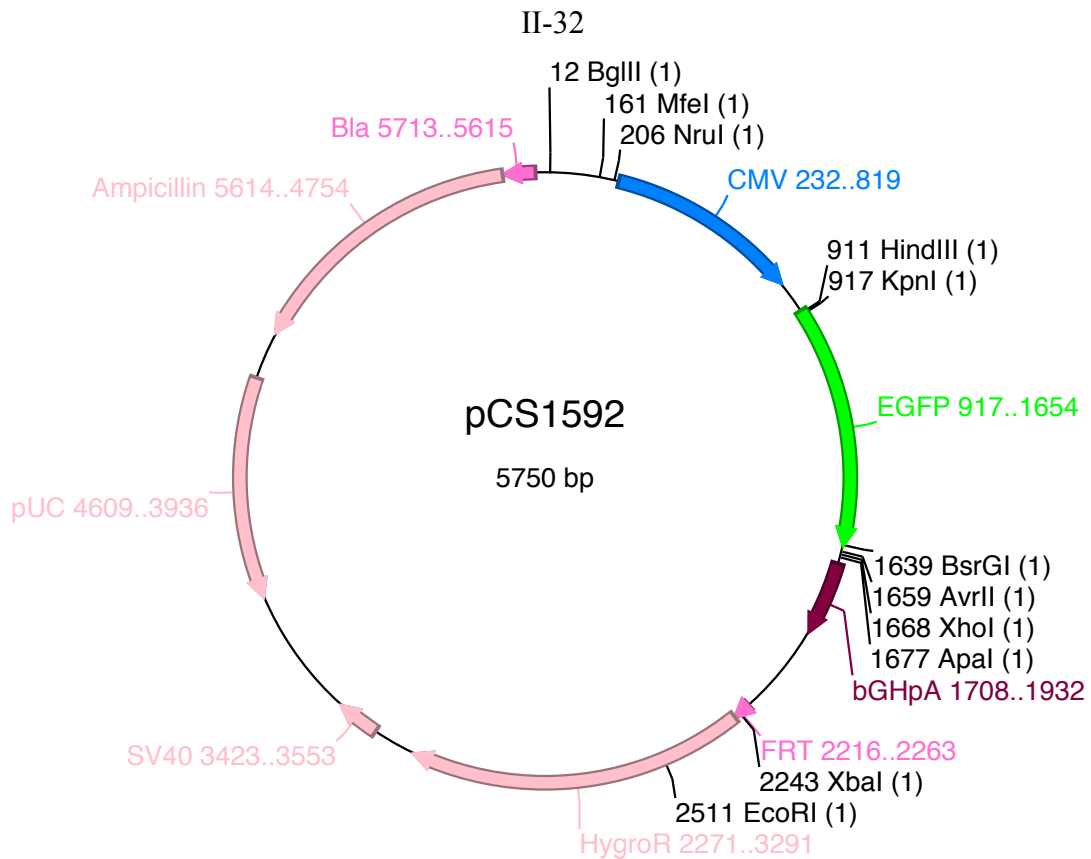


Figure 2.10. Plasmid maps.

The plasmid d2EGFP-Flp-In (courtesy Ryan Bloom) (derived from pcDNA5/FRT (Life Technologies)) was digested with NruI/EcoRV and blunt-end ligated to form pCS2129 (Figure 2.10), which contained DsRed-Express as a transfection control. Trans-ribozymes with tRNA^{Val} 5' and 3' sequences were inserted into pCS2129 between BglII/MfeI.

The DNA fragment insertAvrII was inserted into pCS1302 (courtesy Yvonne Chen) (derived from pcDNA5/FRT) between AvrII/ApaI to form pCS1592 (Figure 2.10), which contained a CMV promoter expressing EGFP. Trans-ribozyme target sequences in one or multiple copies with spacers were digested out of pCS1306 and pCS1642 (sTRSV), pCS1305 and pCS1495 (PLMVd), and pCS1492 and pCS1496 (yEGFP)

(courtesy Kate Galloway) and inserted into pCS1592 using AvrII/XhoI. CU LsIII and HIV target sequences were inserted into pCS1592 between AvrII/XhoI to form pCS1966 and pCS2603, respectively. The coding region of d2EGFP was PCR amplified from the plasmid d2EGFP-Flp-In using the primers d2eGFP HindIII 62 F and d2eGFP AvrII 62 R and inserted into pCS1966 between HindIII/AvrII to form pCS2147. The resulting plasmids were used to create isogenic stable cell lines through the Flp-In system (Life Technologies).

Type I ribozymes with spacers were inserted into pCS1036, which contained a CMV promoter expressing EGFP and DsRed-Express as a transfection control, between XhoI/ApaI (Figure 2.10).

Human cell culture

Flp-In HEK293 cells (Life Technologies) were cultured in 10 mL (10 cm dish) or 3 mL (6 cm dish) Dulbecco's Modified Eagle's medium (DMEM) (Life Technologies) supplemented with 10% fetal bovine serum (FBS) (Life Technologies) and 100 mg/L zeocin (Life Technologies) in a humidified incubator at 37°C and 5% CO₂. Cells were seeded at 2x10⁴ cells/mL and passaged regularly using 0.25% trypsin-EDTA (Life Technologies), with media replaced every 48–72 hours. Cells stably integrated with Flp-In constructs were cultured similarly, except the cell culture media were supplemented with 100 mg/L hygromycin B (Life Technologies) and no zeocin.

Stable cell line generation

Flp-In HEK293 cells were seeded at 1×10^5 cells/mL in 2 mL (6-well plate) DMEM with 10% FBS. 24 hours later the cells were cotransfected with a pcDNA5/FRT-derived plasmid and pOG44 (Life Technologies) in a 1:9 ratio using FuGENE 6 or FuGENE HD (Promega) according to the manufacturer's instructions. Typically DNA and FuGENE were incubated together in Opti-MEM in a 1:3:50 (g:L:L) ratio for approximately 1 hour, with 2 mL samples receiving 2 μ g of DNA. 24 hours after transfection the cells were resuspended using 0.25% trypsin-EDTA and DMEM with 10% FBS, and $\frac{1}{4}$ of the cells were used to seed 2 mL (6-well plate) DMEM with 10% FBS. 24 hours later the media were replaced with DMEM with 10% FBS and 200 mg/L hygromycin B. The media were replaced every 72–96 hours until macroscopic colonies were visible, usually after 10–14 days. Colonies were pooled together with 0.25% trypsin-EDTA and passaged into DMEM with 10% FBS and 100 mg/L hygromycin B. 10% dimethyl sulfoxide (DMSO) stocks were made from resuspended cells, cooled by 1 degree/minute to -80°C , then stored at -320°C .

Transient transfection

Flp-In HEK293 cells were seeded at 1×10^5 or 3×10^5 cells/mL in 500 μ L (24-well plate) DMEM with 10% FBS. 23–29 hours after seeding the cells were transfected with plasmid using FuGENE 6 or FuGENE HD according to the manufacturer's instructions. Typically DNA and FuGENE were incubated together in Opti-MEM in a 1:3:50 (g:L:L) ratio for approximately 1 hour, with 500 μ L samples receiving 500 ng of DNA.

Flow cytometry

40–48 after transfection fluorescence data were obtained by flow cytometry using the Quanta Cell Lab Flow Cytometer equipped with a 488 nm laser (Beckman Coulter). Viability was gated by side scatter and electronic volume, and viable cells were further gated for DsRed expression, which served as a transfection control. GFP and DsRed fluorescence was measured through 525/30 nm band-pass and 610 nm long-pass filters, respectively. Data were analyzed using FlowJo (Tree Star Inc.). Geometric mean values from biological replicates were reported with an error range of ± 1 standard deviation. Geometric mean fluorescence values were normalized to those of a control with no ribozyme or an inactive ribozyme.

***In vitro* cleavage assays**

The CU LsIII trans-ribozyme and its target strand were amplified by PCR from plasmids pCS1949 and pCS1966, respectively, using the primers CU HP T7 F and CU HP T7 R for the ribozyme strand and the primers Barcode T7 F and Barcode T7 R for the target strand. The forward primers added the T7 promoter sequence. Trans-ribozyme RNA was generated by *in vitro* transcription using 1 μ g PCR product DNA as a template, with 40 mM Tris-HCl, pH 7.9, 16 mM MgCl₂, 10 mM dithiothreitol (DTT), 2 mM spermidine, 3 mM rATP, rCTP, rGTP, and rUTP, 40 U RNaseOUT (Life Technologies), and 50 U T7 RNA polymerase (New England Biolabs) in 25 μ L total volume and incubated at 37°C for approximately 2 hours. The transcription product was treated with 2 U of DNaseI (New England Biolabs) at 37°C for approximately 15 min and purified using the RNA Clean & Concentrator-25 kit (Zymo Research) according to the

manufacturer's instructions. Internally radiolabeled target strand RNA was generated by *in vitro* transcription using a similar method, except with rGTP reduced to 300 μ M and supplemented with 5 μ Ci [α - 32 P]rGTP.

Trans-ribozyme and radiolabeled target RNA were denatured separately by heating to 95°C in 50 mM Tris-HCl and 100 mM NaCl, then cooled by 1.2°C/minute to 37°C. Trans-ribozyme (1 μ M final concentration) was added to target (100 nM final concentration) and the reaction was initiated by adding MgCl₂ (500 μ M final concentration) and incubating at 37°C. Aliquots were removed and quenched with RNA stop/load buffer (95% formamide, 30 mM EDTA, 0.25% bromophenol blue, 0.25% xylene cyanol) on ice. Reaction products were heated to 95°C for 5 min, snap cooled on ice for 5 min, and separated by 12% (w/v) denaturing polyacrylamide gel electrophoresis (PAGE) with 8.3M urea. The 32 P radioactivity of cleaved and uncleaved bands was quantified by phosphorimager analysis using a Molecular Imager FX (Bio-Rad Laboratories) and Quantity One software (Bio-Rad Laboratories).

Acknowledgements

We thank Kate Galloway for design of the initial trans-ribozymes and providing plasmid constructs, and Ryan Bloom and Yvonne Chen for providing plasmid constructs. This work was supported by the National Institutes of Health (grant to Christina Smolke, RC1GM091298).

References

1. Guerrier-Takada, C. et al. Phenotypic conversion of drug-resistant bacteria to drug sensitivity. *Proc. Natl. Acad. Sci. U. S. A.* **94**, 8468–8472 (1997).
2. Sarver, N. et al. Ribozymes as potential anti-HIV-1 therapeutic agents. *Science*. **247**, 1222–1225 (1990).
3. Gu, S. et al. Inhibition of infectious human immunodeficiency virus type 1 virions via lentiviral vector encoded short antisense RNAs. *Oligonucleotides* **16**, 287–295 (2006).
4. Carbonell, A. et al. Trans-cleaving hammerhead ribozymes with tertiary stabilizing motifs: in vitro and in vivo activity against a structured viroid RNA. *Nucleic Acids Res.* **39**, 2432–2444 (2011).
5. Hampel, A. The Hairpin Ribozyme: Discovery, Two-Dimensional Model, and Development for Gene Therapy. *Prog. Nucleic Acid Res. Mol. Biol.* **58**, 1–39 (1998).
6. Yu, M. et al. Intracellular immunization of human fetal cord blood stem/progenitor cells with a ribozyme against human immunodeficiency virus type 1. *Proc. Natl. Acad. Sci. U. S. A.* **92**, 699–703 (1995).
7. McCaffrey, A. P. et al. Inhibition of hepatitis B virus in mice by RNA interference. *Nat. Biotechnol.* **21**, 639–644 (2003).
8. Kuwabara, T. et al. A novel allosterically trans-activated ribozyme, the maxizyme, with exceptional specificity in vitro and in vivo. *Mol. Cell* **2**, 617–627 (1998).
9. Kato, Y. et al. Relationships between the activities in vitro and in vivo of various kinds of ribozyme and their intracellular localization in mammalian cells. *J. Biol. Chem.* **276**, 15378–15385 (2001).
10. Zhang, Z. et al. The ABCC4 gene is a promising target for pancreatic cancer therapy. *Gene* **491**, 194–199 (2012).
11. Zhou, W. et al. ShRNA silencing glycogen synthase kinase-3 beta inhibits tumor growth and angiogenesis in pancreatic cancer. *Cancer Lett.* **316**, 178–186 (2012).
12. Michienzi, A. et al. Ribozyme-mediated inhibition of HIV 1 suggests nucleolar trafficking of HIV-1 RNA. *Proc. Natl. Acad. Sci. U. S. A.* **97**, 8955–8960 (2000).
13. Li, M. et al. Inhibition of HIV-1 infection by lentiviral vectors expressing pol III-promoted anti-HIV RNAs. *Mol. Ther.* **8**, 196–206 (2003).

14. Wong-Staal, F. et al. A controlled, Phase 1 clinical trial to evaluate the safety and effects in HIV-1 infected humans of autologous lymphocytes transduced with a ribozyme that cleaves HIV-1 RNA. *Hum. Gene Ther.* **9**, 2407–2425 (1998).
15. Macpherson, J. L. et al. Long-term survival and concomitant gene expression of ribozyme-transduced CD4+ T-lymphocytes in HIV-infected patients. *J. Gene Med.* **7**, 552–564 (2005).
16. Mitsuyasu, R. T. et al. Phase 2 gene therapy trial of an anti-HIV ribozyme in autologous CD34+ cells. *Nat. Med.* **15**, 285–292 (2009).
17. Culler, S. J. et al. Reprogramming cellular behavior with RNA controllers responsive to endogenous proteins. *Science.* **330**, 1251–1255 (2010).
18. Saito, H. et al. Synthetic human cell fate regulation by protein-driven RNA switches. *Nat. Commun.* **2**, 160 (2011).
19. Chang, A. L. et al. Synthetic RNA switches as a tool for temporal and spatial control over gene expression. *Curr. Opin. Biotechnol.* **23**, 679–688 (2012).
20. Liu, Y. et al. Synthesizing oncogenic signal-processing systems that function as both “signal counters” and “signal blockers” in cancer cells. *Mol. Biosyst.* **9**, 1909–1918 (2013).
21. Endo, K. et al. Quantitative and simultaneous translational control of distinct mammalian mRNAs. *Nucleic Acids Res.* **41**, e135 (2013).
22. Buskirk, A. et al. Engineering a ligand-dependent RNA transcriptional activator. *Chem. Biol.* **11**, 1157–1163 (2004).
23. Buzayan, J. M. et al. Nucleotide sequence and newly formed phosphodiester bond of spontaneously ligated satellite tobacco ring spot virus RNA. *Nucleic Acids Res.* **14**, 9729–9743 (1986).
24. Win, M. N. & Smolke, C. D. A modular and extensible RNA-based gene-regulatory platform for engineering cellular function. *Proc. Natl. Acad. Sci. U. S. A.* **104**, 14283–14288 (2007).
25. Liang, J. C. et al. A high-throughput, quantitative cell-based screen for efficient tailoring of RNA device activity. *Nucleic Acids Res.* **40**, e154 (2012).
26. Wei, K. Y. et al. A yeast-based rapid prototype platform for gene control elements in mammalian cells. *Biotechnol. Bioeng.* **110**, 1201–1210 (2013).
27. Chen, Y. Y. et al. Genetic control of mammalian T-cell proliferation with synthetic RNA regulatory systems. *Proc. Natl. Acad. Sci. U. S. A.* **107**, 8531–8536 (2010).

28. Saksmerprome, V. et al. Artificial tertiary motifs stabilize trans-cleaving hammerhead ribozymes under conditions of submillimolar divalent ions and high temperatures. *RNA* **10**, 1916–1924 (2004).
29. Koseki, S. et al. Factors governing the activity in vivo of ribozymes transcribed by RNA polymerase III. *J. Virol.* **73**, 1868–1877 (1999).
30. Bertrand, E. et al. The expression cassette determines the functional activity of ribozymes in mammalian cells by controlling their intracellular localization. *RNA* **3**, 75–88 (1997).
31. Kuwabara, T. et al. Significantly higher activity of a cytoplasmic hammerhead ribozyme than a corresponding nuclear counterpart: engineered tRNAs with an extended 3' end can be exported efficiently and specifically to the cytoplasm in mammalian cells. *Nucleic Acids Res.* **29**, 2780–2788 (2001).
32. Sano, M. et al. Novel method for selection of tRNA-driven ribozymes with enhanced stability in mammalian cells. *Antisense Nucleic Acid Drug Dev.* **12**, 341–352 (2002).
33. Warashina, M. et al. RNA-protein hybrid ribozymes that efficiently cleave any mRNA independently of the structure of the target RNA. *Proc. Natl. Acad. Sci. U. S. A.* **98**, 5572–5577 (2001).
34. Weinberg, M. S. & Rossi, J. J. Comparative single-turnover kinetic analyses of trans-cleaving hammerhead ribozymes with naturally derived non-conserved sequence motifs. *FEBS Lett.* **579**, 1619–1624 (2005).
35. Birikh, K. R. et al. The structure, function and application of the hammerhead ribozyme. *Eur. J. Biochem.* **245**, 1–16 (1997).
36. Khvorova, A. et al. Sequence elements outside the hammerhead ribozyme catalytic core enable intracellular activity. *Nat. Struct. Biol.* **10**, 708–712 (2003).
37. Kennedy, A. B. et al. A versatile cis-blocking and trans-activation strategy for ribozyme characterization. *Nucleic Acids Res.* **41**, e41 (2013).
38. Wieland, M. et al. Expanded hammerhead ribozymes containing addressable three-way junctions. *RNA* **15**, 968–976 (2009).
39. Koizumi, M. et al. Cleavage of specific sites of RNA by designed ribozymes. *FEBS Lett.* **239**, 285–288 (1988).
40. Uhlenbeck, O. C. A small catalytic oligoribonucleotide. *Nature* **328**, 596–600 (1987).

41. Flores, R. et al. Hammerhead ribozyme structure and function in plant RNA replication. *Methods Enzymol.* **341**, 540–552 (2001).
42. Li, X. et al. Generation of Destabilized Green Fluorescent Protein as a Transcription Reporter. *J. Biol. Chem.* **273**, 34970–34975 (1998).
43. Singer, R. H. RNA zipcodes for cytoplasmic addresses. *Curr. Biol.* **3**, 719–721 (1993).
44. Kislauskis, E. H. et al. Sequences responsible for intracellular localization of beta-actin messenger RNA also affect cell phenotype. *J. Cell Biol.* **127**, 441–451 (1994).
45. Beisel, C. L. et al. Design of small molecule-responsive microRNAs based on structural requirements for Drosha processing. *Nucleic Acids Res.* **39**, 2981–2994 (2011).
46. Qi, L. S. et al. Repurposing CRISPR as an RNA-guided platform for sequence-specific control of gene expression. *Cell* **152**, 1173–1183 (2013).

Supplementary Tables

Supplementary Table 2.1. Primer and oligonucleotide sequences.

Name	DNA sequence
insertFseI	AAAGGCCGGCCAAA
insertAvrII	AAACTCGAGAAA
sTRSV trans	ATCCTCCAATCCTTTAGCTTTGACTCCTGATGAGTGGGTGA CCACGAAACTGATGAC
sTRSV target sequence	GTCATCAGTCGAGTCATACTAAAGGATAGGAGGAAT
PLMVd trans	TCTTACTGAATTTACCTAACCCCACTGATGAGTCGCTGAAA TGCGACGAAACTTTGCTT
PLMVd target sequence	AAGCAAAGTCTGGGGGGTAAATATCAAGTAAGA
yEGFP trans	AGCAGTAACAAATTCTTAAAACAACCTGATGAGTCGCTGAA ATGCGACGAAACCATGTG
yEGFP target sequence	CACATGGTCTTGTTAGAATTTGTTACTGCT
CU LsIII trans	ATCCTCCAATCCTTTATTTCCGGTCTGATGAGTCCGTGAGG ACGAAACAGCTGAC
CU LsIII ctrl trans	ATCCTCCAATCCTTTATTTCCGGTGTACTGTGTCCGTGAGG ACCGAACAGCTGAC
CU LsIII target sequence	GTCAGCTGTCACCGGATGTGCTAAAGGATAGGAGGA
HIV trans	ACACAACACTGATGAGGACCGAAAGGTCCGAAACGGGCAC
HIV ctrl trans	ACACAACACTAATGAGGACCGAAAGGTCCGAAACGGGCAC
HIV target sequence	GTGCCCGTCTGTTGTGT
target sequence 5' spacer	TAAATCTAGGAAACAAA
target sequence 3' spacer	ATAAACAAACTCGATCCGCGAAAAAACCGCGGA
U6 trans-ribozyme cassette	GTCTGTACAGGTGTCTTCTTGAGCATGCTCAAGAGACATTA ATTAAACAACCGGTACGTCCATTACAAAGTAATGGACGTG GCGCGCCGATATCGATAAATTTTTTAAA
CMV trans-ribozyme cassette	GGTGTCTTCTTGAGCATGCTCAAGAGACATTAATTAACAA CCGGTACGTCCATTACAAAGTAATGGACGT
ancillary large hairpin U6 5'	GTGTCACCTGCAGTATTAGCAAATAATACATGCAAGTGAC
ancillary large hairpin U6 3' and CMV	GTCACCTGCAGTATTAGCAAATAATACATGCAAGTGAC

ancillary cis-ribozyme 5'	AAACAAAATCCTTTATTTCCGGTCTGATGAGTCCGTGAGGACGAAACAGCTGACAAAAGTCAGCTGTCACCGGATGTGCTA AAGGATAAAAAGA
ancillary cis-ribozyme 3'	AAACAAAGCTGTCACCGGATGTGCTTTCCGGTCTGATGAGTCCGTGAGGACGAAACAGCAAAAAGA
tRNA 5'	AGGACTAGTCTTTTAGGTCAAAAAGAAGAAGCTTTGTAACCGTTGGTTTCCGTAGTGTAGTGGTTATCACGTTTCGCCTAAC ACGCGAAAGGTCCCCGGTTCGAAACCGGGCACTACAA
tRNA 3'	GTCGGAAACGGTTTTTTTTCTATCGCGTCGAC
sTRSVctrl	GCTGTCACCGGATGTGCTTTCCGGTACGTGAGGTCCGTGAGGACAGAACAGC
sTRSV	GCTGTCACCGGATGTGCTTTCCGGTCTGATGAGTCCGTGAGGACGAAACAGC
K	ATCCTTTAGCTTTGACTCCTGATGAGTGGGTGACCACGAAACTGATGACGTTGGTCATCAGTCGAGTCATACTAAAGGAT
W	ATCCTTTAGCTTTCCGGTCTGATGAGTCCGTGAGGACGAAACAGCAAAAGCTGTCACCGGATACTAAAGGAT
Y	ATCCTTTAGCTTTCCGGTCTGATGAGTCCGTGAGGACGAAACAGCAAAAGCTGTCACCGGATGTTAAAGGAT
CU	ATCCTTTATTTCCGGTCTGATGAGTCCGTGAGGACGAAACAGCAAAAGCTGTCACCGGATGTGCTAAAGGAT
CU LsIII	ATCCTTTATTTCCGGTCTGATGAGTCCGTGAGGACGAAACAGCTGACAAAAGTCAGCTGTCACCGGATGTGCTAAAGGAT
CU LsIII inversion	ATCCTTTATTTCCGGTCTGATGAGTCCGTGAGGACGAAACTGCTGACAAAAGTCAGCAGTCACCGGATGTGCTAAAGGAT
CK LsI	ATCCTTTATTTGACTCCTGATGAGTCCGTGAGGACGAAACAGCTGACAAAAGTCAGCTGTCGAGTCATGTGCTAAAGGAT
CK LsIII	ATCCTTTATTTCCGGTCTGATGAGTCCGTGAGGACGAAACTGATGACAAAAGTCATCAGTCACCGGATGTGCTAAAGGAT
CK LsIV	ATCCTTTATTTGACTCCTGATGAGTCCGTGAGGACGAAACTGATGACAAAAGTCATCAGTCGAGTCATGTGCTAAAGGAT
U LsIII	ATCGAATATGTGCTTTCCGGTCTGATGAGTCCGTGAGGACGAAACAGCTGACAAAAGTCAGCTGTCACCGGATATTCGAT
HHe-PLMVd	GTGGTTCATAACACCTCTGATGAGTCGCTGAAATGCGACGAAACCTCCTGAGCAAAAGCTCAGGAGGTCAGGTGTGAACCA C
3-way AA	GGGATCAGTAAGGATGTGCTTTCCGGTCTGATGAGTCCGTGAGGACGAAACAGCTGACAAAAGTCAGCTGTCACCACTGAT CCC
3-way AAA	GGGATCAGTAAAGGATGTGCTTTCCGGTCTGATGAGTCCGTGAGGACGAAACAGCTGACAAAAGTCAGCTGTCACCACTGAT TCCC
A 5' spacer	AAACAAACAAA
A 3' spacer	AAAAGAAAATAAAAATTTTTTGAA
B 5' spacer	AATAAATAAAA

B 3' spacer	CAAATAAACAAACACTC
d2eGFP HindIII 62 F	TAGAAGCTTATGGTGAGCAAGGGCGAGGAG
d2eGFP AvrII 62 R	AAGCCTAGGTTTTGCTACACATTGATCCTAGCAGAAGCACAGG
CU HP T7 F	TTCTAATACGACTCACTATAGGGTGTCTTCTTGAGCATGCTCAAGAGACATTAATTAATCCTC
CU HP T7 R	ACGTCCATTACTTTGTAATGGACGTACCGGTG
Barcode T7 F	TTCTAATACGACTCACTATAGGACAAGTAACTCGAAAAACCTAGGTAAATCTAGGAAACAAAGT
Barcode T7 R	CTTCTCGAGTCCGCGGTTTTTTCGC

Supplementary Table 2.2. Plasmid constructs.

Plasmid	Description
pCS1592	pCS1302 with insertAvrII inserted between AvrII/ApaI
pCS1631	pCS1592 with sTRSV target sequence with spacers inserted between AvrII/XhoI
pCS1632	pCS1592 with sTRSV target sequence (4 copy) with spacers inserted between AvrII/XhoI
pCS1629	pCS1592 with PLMVd target sequence with spacers inserted between AvrII/XhoI
pCS1630	pCS1592 with PLMVd target sequence (4 copy) with spacers inserted between AvrII/XhoI
pCS1633	pCS1592 with yEGFP target sequence with spacers inserted between AvrII/XhoI
pCS1634	pCS1592 with yEGFP target sequence (4 copy) with spacers inserted between AvrII/XhoI
pCS1966	pCS1592 with CU LsIII target sequence with spacers inserted between AvrII/XhoI
pCS2063	pCS1592 with HIV target sequence with spacers inserted between AvrII/XhoI
pCS1576	pCS1036 with insertFseI inserted between KpnI/XhoI
pCS1646	pCS1576 with U6 trans-ribozyme cassette inserted between BamHI/EcoRI
pCS1662	pCS1576 with CMV trans-ribozyme cassette inserted between FseI/XhoI
pCS1655	pCS1646 with sTRSV trans inserted between PacI/AgeI
pCS1653	pCS1646 with PLMVd trans inserted between PacI/AgeI
pCS1657	pCS1646 with yEGFP trans inserted between PacI/AgeI
pCS1685	pCS1662 with sTRSV trans inserted between PacI/AgeI

pCS1683	pCS1662 with PLMVd trans inserted between PacI/AgeI
pCS1687	pCS1662 with yEGFP trans inserted between PacI/AgeI
pCS1949	pCS1662 with CU LsIII trans inserted between PacI/AgeI
pCS1955	pCS1662 with ancillary cis-ribozyme 5' inserted between HindIII/KpnI and ancillary cis-ribozyme 3' inserted between XbaI/ApaI
pCS1956	pCS1662 with ancillary cis-ribozyme 5' inserted between HindIII/KpnI, ancillary cis-ribozyme 3' inserted between XbaI/ApaI, and ancillary large hairpin U6 3' and CMV inserted between KpnI/FseI and XhoI/XbaI
pCS1954	pCS1662 with ancillary large hairpin U6 3' and CMV inserted between KpnI/FseI and XhoI/XbaI
pCS1953	pCS1646 with ancillary large hairpin U6 5' inserted between BamHI/BsrGI and ancillary large hairpin U6 3' and CMV inserted between AscI/ClaI
pCS2012	pCS1955 with CU LsIII trans inserted between PacI/AgeI
pCS2013	pCS1955 with CU LsIII ctrl trans inserted between PacI/AgeI
pCS2014	pCS1956 with CU LsIII trans inserted between PacI/AgeI
pCS2015	pCS1956 with CU LsIII ctrl trans inserted between PacI/AgeI
pCS2010	pCS1954 with CU LsIII trans inserted between PacI/AgeI
pCS2011	pCS1954 with CU LsIII ctrl trans inserted between PacI/AgeI
pCS2008	pCS1953 with CU LsIII trans inserted between PacI/AgeI
pCS2009	pCS1953 with CU LsIII ctrl trans inserted between PacI/AgeI
pCS2129	pcDNA5/FRT with DsRed-Express inserted between BamHI/AgeI
pCS2059	pCS2129 with tRNA 5' - CU LsIII trans - tRNA 3' inserted between BglII/MfeI
pCS2060	pCS2129 with tRNA 5' - CU LsIII ctrl trans - tRNA 3' inserted between BglII/MfeI
pCS2061	pCS2129 with tRNA 5' - HIV trans - tRNA 3' inserted between BglII/MfeI
pCS2062	pCS2129 with tRNA 5' - HIV ctrl trans - tRNA 3' inserted between BglII/MfeI
pCS1820	pCS1036 with sTRSVctrl with A spacers inserted between XhoI/ApaI
pCS1819	pCS1036 with sTRSV with A spacers inserted between XhoI/ApaI
pCS1816	pCS1036 with K with A spacers inserted between XhoI/ApaI
pCS1817	pCS1036 with W with A spacers inserted between XhoI/ApaI
pCS1818	pCS1036 with Y with A spacers inserted between XhoI/ApaI
pCS2080	pCS1036 with CU with B spacers inserted between XhoI/ApaI
pCS2081	pCS1036 with CU LsIII with B spacers inserted between XhoI/ApaI
pCS2083	pCS1036 with CU LsIII inversion with B spacers inserted between XhoI/ApaI
pCS1930	pCS1036 with CK LsI with A spacers inserted between XhoI/ApaI
pCS1931	pCS1036 with CK LsIII with A spacers inserted between XhoI/ApaI
pCS1932	pCS1036 with CK LsIV with A spacers inserted between XhoI/ApaI
pCS2085	pCS1036 with U LsIII with B spacers inserted between XhoI/ApaI
pCS2087	pCS1036 with HHe-PLMVd with B spacers inserted between XhoI/ApaI

pCS2088	pCS1036 with 3-way AA with B spacers inserted between XhoI/ApaI
pCS2089	pCS1036 with 3-way AAA with B spacers inserted between XhoI/ApaI
pCS2147	pCS1966 with d2EGFP inserted between HindIII/AvrII

Supplementary Table 2.3. Human cell lines with stably integrated constructs.

Parental line	Integrated plasmid construct
Flp-In HEK293	pCS1631
Flp-In HEK293	pCS1632
Flp-In HEK293	pCS1629
Flp-In HEK293	pCS1630
Flp-In HEK293	pCS1633
Flp-In HEK293	pCS1634
Flp-In HEK293	pCS1966
Flp-In HEK293	pCS2063